
GENERAL EXPERIMENTAL
TECHNIQUES

A Source of Radially Converging Low-Energy High-Current Electron Beams

P. P. Kiziridi^{a,*} and G. E. Ozur^{a,**}

^a Institute of High Current Electronics, Siberian Branch, Russian Academy of Sciences,
Tomsk, 634055 Russia

*e-mail: kiziridi_pavel@mail.ru

**e-mail: ozur@lve.hcei.tsc.ru

Received April 27, 2022; revised June 6, 2022; accepted July 4, 2022

Abstract—The design and some characteristics of a source of radially converging low-energy (5–25 keV) high-current electron beams of microsecond pulse duration, which is aimed at surface modification of cylindrical parts and samples, are presented. The cathode unit of the source is a duralumin ring with an 8-cm inner diameter in which 18 resistively decoupled arc plasma sources are built-in. The operability of the source electron gun in the vacuum-diode (with a residual-gas pressure of ~0.013 Pa) and gas-filled-diode modes at pressures of 0.05–0.09 Pa has been demonstrated. The beam energy density on the 1-cm-diameter anode is sufficient for surface melting of copper (the threshold of pulsed copper melting is 5–5.5 J/cm² at a pulse duration of 2–3 μs) at a 17-kV charging voltage of the high-voltage pulse generator that powers the electron gun.

DOI: 10.1134/S0020441222060124

INTRODUCTION

Low-energy (10–30 keV) high-current (up to 25 kA) electron beams (LHEBs) have been widely used to modify the surface layers of metallic materials for several decades [1–6]. The formation of such beams is usually performed in guns with a plasma anode and a multiemitter explosive-emission cathode [7, 8]. The high energy density (up to 20 J/cm²) and the short pulse duration (2–4 μs) make it possible to release a significant beam energy in a thin (fractions–units of microns) surface layer, thus bringing it to melting and even partial evaporation. This makes it possible to develop various promising technologies, including the formation of surface alloys with a thickness of fractions to tens of microns [1–7].

The electron guns of LHEB sources that have been created to date have a planar–axial geometry and form, as a rule, cylindrical beams transported along the lines of force of an external guide magnetic field [7, 8]. This field also provides the ignition of a high-current reflective (Penning) discharge (usually in argon) that forms the plasma anode of an electron gun. In this case, the electrodes of the discharge cell are an explosive-emission cathode, a collector, and an annular anode located approximately in the middle between them. At the same time, there are many tasks when it is required to irradiate extended cylindrical products; for this purpose, it is most reasonable to use radially converging beams. Such tasks include the formation of protective coatings for the shells of fuel elements of

nuclear reactors, which are made mainly of zirconium alloys or alloy steels, to prevent or slow down corrosion and high-temperature oxidation; increasing the lifetime of various cutting and stamping tools. The absence of electron guns with radially converging LHEB determines the relevance of their development and creation.

Pulsed radially converging electron beams were used and are used at present for a wide variety of purposes. These are pumping of gas lasers [9], generation of microwave radiation [10, 11], and, certainly, modifying the surface layers of materials [12, 13]. Almost all of the above-mentioned installations generate high-energy beams (~100 keV and higher) with a relatively small current density (units–tens of amperes per square centimeter). The installations of the GESA series developed at the Efremov Research Institute of Electrophysical Apparatus (St. Petersburg) are the closest in purpose to our LHEP sources [12, 13].

In [12], a radially converging electron beam was generated in a triode-type gun with a cathode diameter of 28 cm and a grid diameter of 20 cm. The axial length of the cathode and grid was 35 cm, while the cathode surface area was 2900 cm². The total number of emitters (graphite fiber bundles) on the cathode was 2815; a resistor with a resistance of several kilohm is connected in series to the circuit of each emitter. The anode diameter varied and was 1, 2, or 3 cm. A high-voltage generator of rectangular pulses with durations of up to 30 μs provided an accelerating voltage between

the cathode and anode with an amplitude of 100–120 kV. The beam current to the anode reached 2–5 kA.

Experiments and calculations performed in [12] revealed the following negative effect. Due to the angular spread for $\sim 10^\circ$ from the beginning of a pulse, a significant part of beam electrons does not fall on the anode and oscillates in the cathode–anode space; with a decrease in the anode diameter, the fraction of oscillating electrons increases (the anode current certainly decreases), the pulse duration decreases, and the stability of the gun operation deteriorates. Moreover, electron oscillations and the resulting accumulation of a negative volume charge increase the deviation of electrons from hitting the anode and even led to a decrease in the cathode emission current in [12], which correlates with the results from [14].

The authors of [12] partially overcame this drawback in study [13] on the GESA-4 installation. To reduce the angular spread between the grid and the anode, thin plates (lamellae) were installed radially, whose length (in the axial direction) was equal to the cathode length. The fraction of oscillating electrons decreased, and the gun operated more stably.

However, a significant disadvantage of GESA series installations is a relatively high accelerating voltage (up to 250 kV), which leads to expensive equipment and reduces its reliability. In addition, achieving the required beam energy density due to the pulse duration (due to the low current density) urged the authors of [12, 13] to use large (~ 10 cm) interelectrode radial gaps, which led to oscillations of a significant part of the beam electrons that do not hit the anode. It should also be noted that even with such interelectrode gaps, their breakdown was often observed in [12, 13] due to the gas emission from the anode under the beam action. To prevent breakdowns, the authors had to warm up the anode to 400–500°C with a special pulsed current source before the start of a beam pulse, which led to additional costs. Nevertheless, due to a higher current density, a lower (by several times!) accelerating voltage, and unnecessary preliminary anode heating, LHEB sources seem more promising to us. This paper describes the MicrEB source (microsecond electron beam) with a radially converging LHEB we developed.

DESCRIPTION OF THE SOURCE

To form a radially converging LHEB, we used a cathode unit with multichannel initiation of the explosive emission by a breakdown over the dielectric surface, which was recently developed [15, 16]. Figure 1 shows a general view of the source's electron gun. Eighteen arc plasma sources that include tubes 2 and copper electrodes 3 are built in a single-section annular duralumin cathode 1 uniformly around its circumference. The inner diameter of the cathode is 8 cm, the outer diameter of the tubes is 4 mm, their inner diam-

eter is 2 mm, and the diameter of the electrodes is also 2 mm. Each of the 18 electrodes is grounded through resistors 4 (three series-connected resistors with a nominal resistance of 750 Ω each). To increase the number of explosive-emission centers, 12 bundles of thin (80 μm) copper wires 5 are also pressed into the ring.

The gun operates as follows. When a voltage pulse of negative polarity with an amplitude of 5–25 kV is applied to the cathode from a high-voltage pulse generator (HVPG), a breakdown occurs along the surface of the ends of ceramic tubes 2 and plasma is produced that consists of the materials of the cathode (cathode spots), ceramic tubes, and electrodes 3, as well as of ionized desorbed gas. The formation of cathode spots (explosive-emission centers) during the current flow through the igniting gaps (these spots can be called seed) is provided by the fact that the current amplitude (2.2–11.1 A) through each gap exceeds the so-called threshold arc current [17], which amounts to fractions—units of amperes for almost all materials (e.g., it is ~ 2 A for copper). The electrons emitted by seed spots, as well as by the cathode spots that have arisen during the pulse, are accelerated radially towards the anode, thus forming a converging beam. The current rise is provided by both an increase in the number of cathode spots and their expansion, i.e., an increase in the emission-surface area [7, 18].

Anode 6 is a stainless-steel or brass rod with a diameter of 1 cm. In some cases, a part of the anode (the area exposed to the beam) was wrapped with a 0.5-mm-thick copper foil (see below, Fig. 5c). The anode is grounded on both sides through collet current collectors 8 and 9.

The HVPG (its circuit is shown in Fig. 2) is built on the basis of an IK-50/3 capacitor (the measured capacitance is $C = 2.87 \mu\text{F}$) and a TD-50k/45 pseudo-spark switch (OOO Impul'snye tekhnologii, Ryazan). An inductive–resistive coil L_2, R_2 , which is wound with a 1-mm-thick nichrome wire, is intended to close the charging and capacitor-energy absorbing circuit in the case of an idle stroke in the load as well as to protect the output circuits of the HVPG charging source. The ohmic resistance of the coil is 23.5 Ω and the design inductance is 140 μH . The HVPG is connected to the electron gun through a transmission line of six parallel segments of an RK-50-9-11 cable with a length of 1.5 m each. The HVPG impedance is 0.25 Ω at most.

The accelerating voltage pulses were registered using an active divider, the total cathode current was recorded with a Rogowsky coil, and the beam current to the anode was also recorded with Rogowsky coils that envelope both current collectors. Signals from the sensors were fed to the inputs of a Tektronix TDS 2024 four-channel broadband (200 MHz) digital oscilloscope. Five shots were performed in each mode.

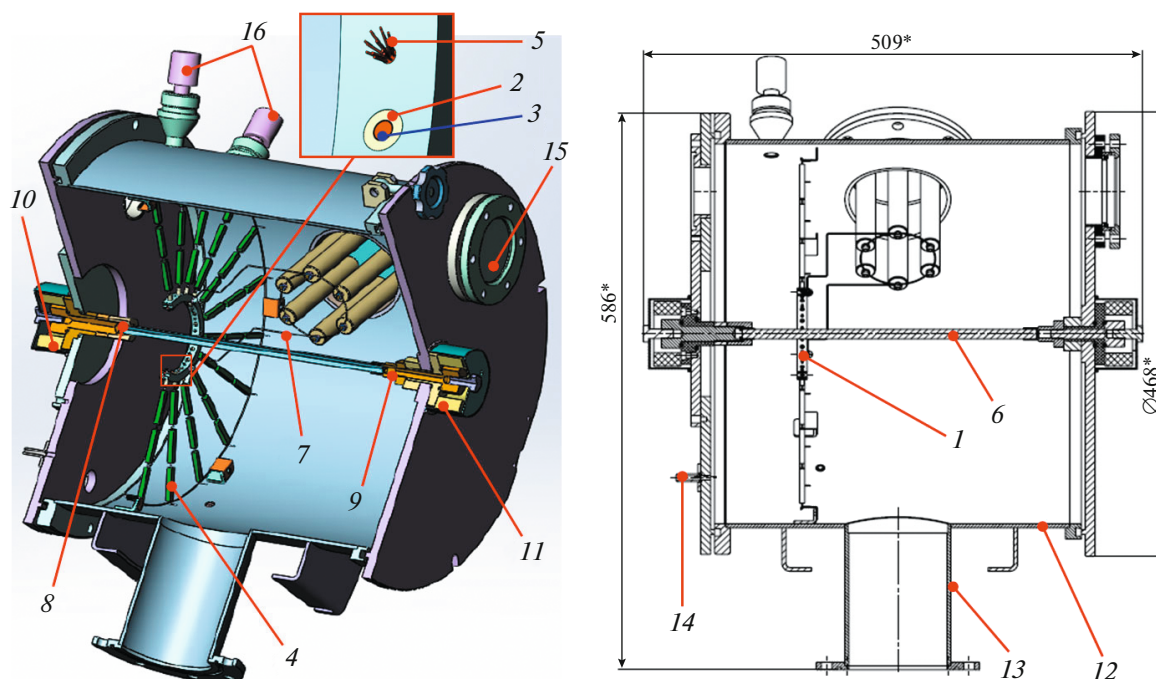


Fig. 1. General view of the working chamber and the electron gun of the LHEB source: (1) cathode; (2) ceramic tube; (3) electrode of the arc plasma source; (4) TVO-2 resistor; (5) copper wire bundle; (6) anode; (7) wires for feeding high-voltage pulses from the transmission line to the cathode; (8, 9) collet current collectors; (10, 11) Rogowsky coils; (12) working chamber; (13) evacuation pipe; (14) pipe for working-gas admission; (15) viewing window with lead glass; and (16) gas-pressure sensors.

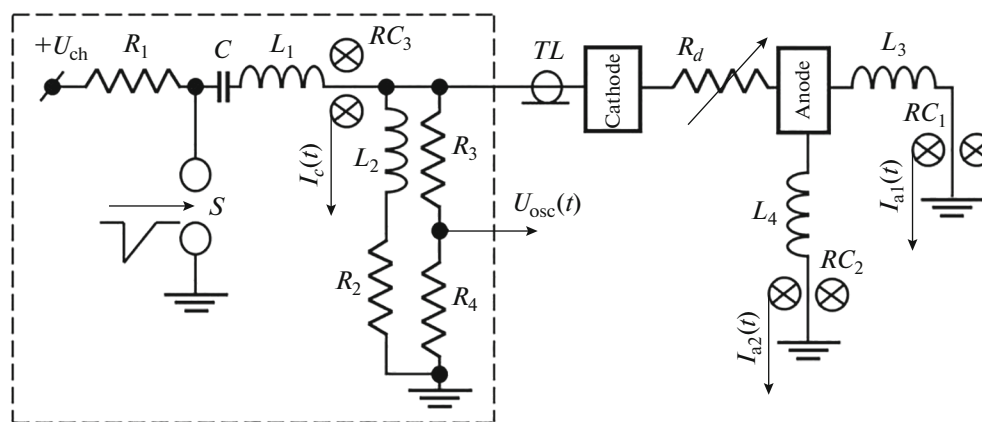


Fig. 2. Schematic diagram of the HVPG (highlighted with a dashed line) and the discharge circuit (circuits of the arc plasma sources are not shown): ($R_1 = 4.7 \text{ k}\Omega$) charging resistor; ($R_2 = 23.5 \Omega$) resistance of the HVPG coil; ($R_3 = 10 \text{ k}\Omega$, $R_4 = 5 \Omega$) voltage divider; (R_d) diode resistance; ($L_1 \approx 120 \text{ nH}$) inductance of the discharge circuit minus the inductances in the anode circuit; ($L_2 \approx 140 \mu\text{H}$) inductance of the HVPG coil; (L_3 , L_4) inductances in the anode circuit; (TL) transmission line; (RC_1 – RC_3) Rogowsky coils (current transformers); and (S) TD-50k/45 controlled switch.

The beam energy density in a pulse and its distribution over the anode surface were evaluated from beam autographs.

Plasma glow was photographed through viewing window 15 (see Fig. 1) using a CASIO QV-3000EX/Ir digital camera in the open-shutter mode. A 3-mm-thick NS-9 interference optical filter (with an index of

absorption of $\alpha\lambda = 0.6$ – 0.65 depending on the wavelength per thickness of 1 mm) was installed in front of the camera lens to avoid excessive illumination.

The working volume of the gun was evacuated with a turbomolecular pump to a pressure of 0.013 Pa; after the evacuation, the working gas was puffed to pressures of 0.05–0.09 Pa.

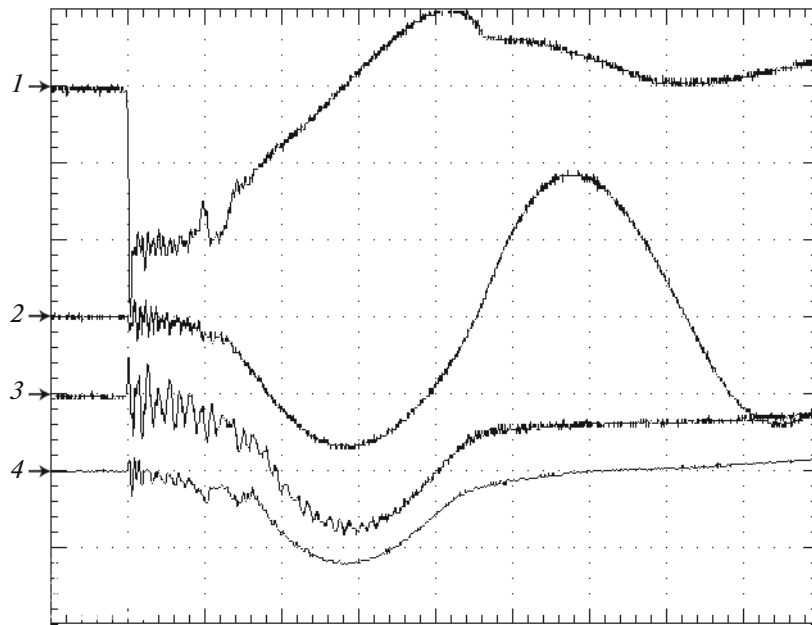


Fig. 3. Typical waveforms of pulses: (1) accelerating voltage (10 kV/div); (2) total cathode current (24 kA/div); (3, 4) beam currents to the anode registered, respectively, with Rogowsky coils RC_2 (5 kA/div) and RC_1 (10 kA/div). The horizontal scale is 1 μ s/div. $U_{ch} = 20$ kV, $p = 0.09$ Pa.

RESULTS AND DISCUSSION

Figure 3 shows typical waveforms of the accelerating voltage pulses (without correction for the inductive voltage drop across the transmission line and feeding conductors), the total current in the circuit, and the currents in the anode circuit. The currents registered in the circuits of the first and second current collectors are different due to the different lengths of the anode segments from the cathode plane to the corresponding current collector and, hence, their different induc-

tances (the design inductances are 76 and 207 nH). At the same time, the ratio of these currents, as a rule, is approximately inversely proportional to the ratio of these inductances. The total beam current to the anode (the sum of the currents recorded with sensors RC_1 and RC_2) is noticeably lower than the total current in the circuit recorded with the sensor RC_3 that is located in the HVPG. This indicates the presence of current leaks through insulators and/or to the chamber wall, which result in a breakdown and a transition

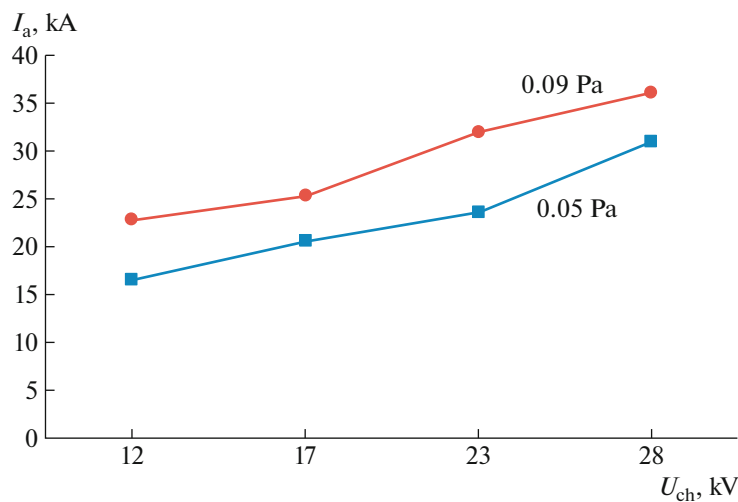


Fig. 4. Dependence of the anode current amplitude on the HVPG charging voltage for different air pressures in the working chamber (figures at the curves).

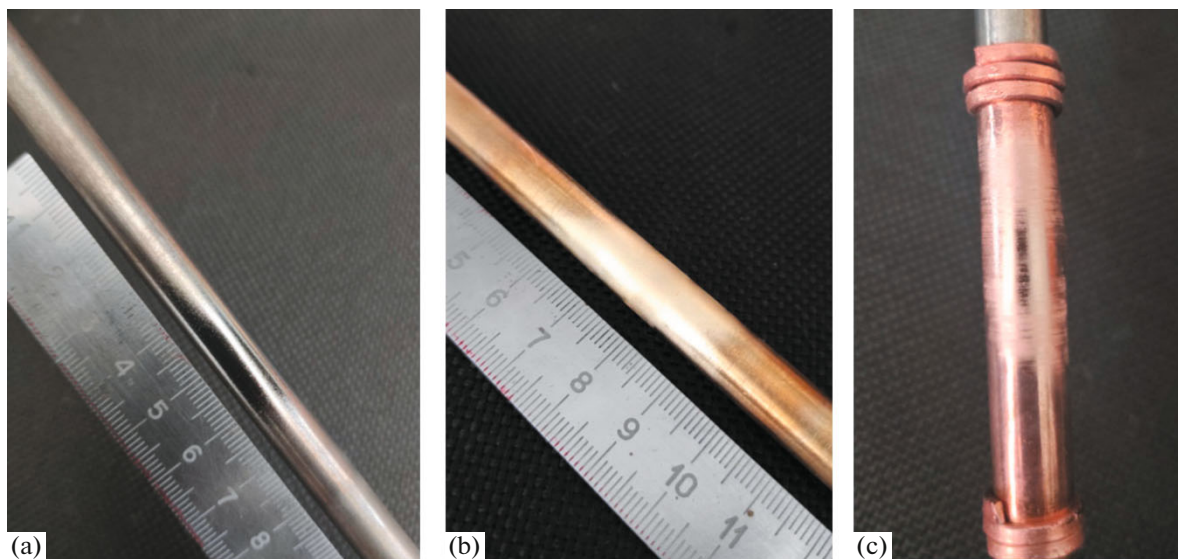


Fig. 5. Beam autographs on (a) stainless steel, (b) brass, and (c) copper; $U_{\text{ch}} = 17$ kV and $p = 0.09$ Pa.

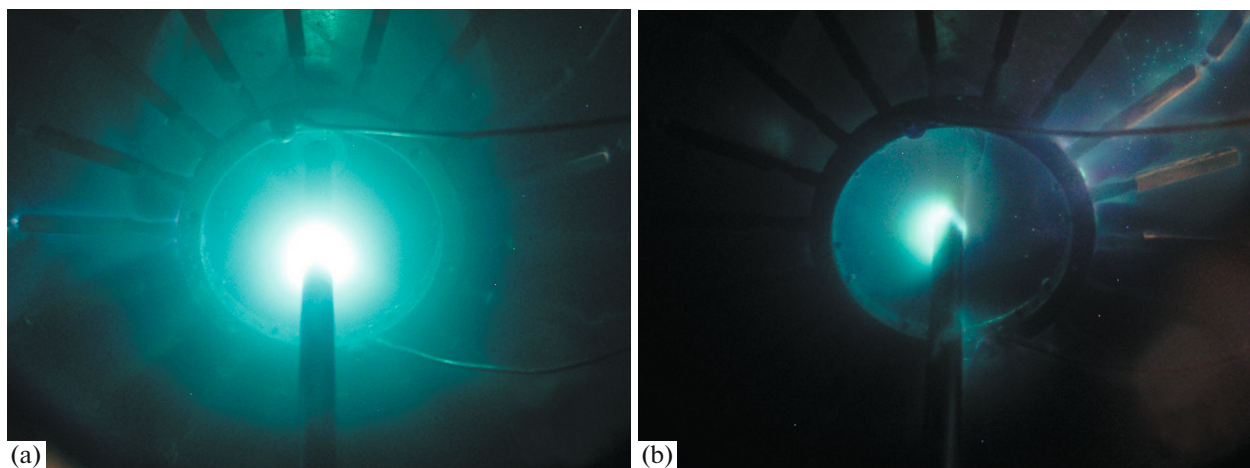


Fig. 6. Photos of glow during operation of the electron gun in the modes: (a) gas-field diode ($p = 0.09$ Pa) and (b) vacuum diode ($p = 0.013$ Pa); $U_{\text{ch}} = 17$ kV.

of the discharge into an oscillatory mode. The waveforms of currents (their time behavior) are close to those obtained for the planar–axial geometry of the diode [16].

Figure 4 shows the dependence of the total beam current to the anode I_a on the charging voltage U_{ch} of the HVPG, i.e., actually on the accelerating voltage. It can be seen that the beam current to the anode increases monotonically with increasing U_{ch} .

Figure 5 shows photos of the anodes after irradiation with LHEB at an air pressure of 0.09 Pa. The autographs produced by the beam show that traces of intense melting are observed in the region close to the plane of the cathode emitters. Considering that the

threshold of pulsed copper melting at a pulse duration of 2–3 μs is 5–5.5 J/cm² [19], it can be assumed that the specified energy density is achieved at a relatively moderate value of $U_{\text{ch}} = 17$ kV. The length of the melted area along the anode axis is 1–2 cm; it is followed by a region of less intense melting (beam halo). Along the circumference of the anode, traces of the beam action look more or less uniform, thus indicating the azimuthal uniformity of the beam. In the vacuum-diode mode (0.013 Pa), the azimuthal uniformity of the beam was sometimes violated, as far as this can be deduced from photos of the anode plasma glow, which was obtained using a digital camera with an open shutter (Fig. 6).

CONCLUSIONS

A MicrEB source of radially converging low-energy (5–25 keV) high-current (up to 30 kA) electron beams with a pulse duration of 2–4 μ s has been created. The source is capable of operating in the mode of a vacuum or gas-filled diode at low working gas pressures (\sim 0.05–0.1 Pa for air) due to resistively decoupled arc plasma sources that are built into the cathode. The source operates more stably in the gas-filled diode version. The energy density of the beam in a pulse reaches at least 5–5.5 J/cm² at a charging voltage of 17 kV of the high-voltage pulse generator feeding the electron gun. This energy density is sufficient to melt the overwhelming majority of metals and alloys. In the azimuthal direction, the beam autograph on the anode looks homogeneous. The further improvement of the source will consist in minimizing the electron-current leakage as well as in expanding the area of homogeneous melting of the anode (target) by adding cathode sections.

ACKNOWLEDGMENTS

We are grateful to V.I. Petrov, A.G. Padei, and I.N. Kononov for their help in this study.

FUNDING

This study was supported by the Russian Science Foundation, project no. 22-29-00070.

CONFLICT OF INTEREST

The authors declare that they have no conflicts of interest.

REFERENCES

1. Meisner, L.L., Markov, A.B., Rotshtein, V.P., Ozur, G.E., Meisner, S.N., Yakovlev, E.V., Semin, V.O., Mironov, Yu.P., Poletika, T.M., Girsova, S.L., and Shepel, D.A., *J. Alloys Compd.*, 2018, vol. 730, p. 376. <https://doi.org/10.1016/j.jallcom.2017.09.238>
2. Rotshtein, V.P. and Shulov, V.A., *J. Metall.*, 2011, vol. 2011, article ID 673685.
3. Uno, Y., Okada, A., Uemura, K., Raharjo, P., Furukawa, T., and Karato, K., *Precis. Eng.*, 2005, vol. 29, no. 4, p. 449. <https://doi.org/10.1016/j.precisioneng.2004.12.005>
4. Ozur, G.E., Proskurovsky, D.I., Rotshtein, V.P., and Markov, A.B., *Laser Part. Beams*, 2003, vol. 21, no. 2, p. 157. <https://doi.org/10.1017/S0263034603212040>
5. Murray, J.W. and Clare, A.T., *J. Mater. Process. Technol.*, 2012, vol. 212, p. 2642. <https://doi.org/10.1016/j.jmatprotec.2012.07.018>
6. Rotshtein, V.P., Proskurovskii, D.I., Ozur, G.E., and Ivanov, Yu.F., *Modifikatsiya poverkhnostnykh sloev metallicheskih materialov nizkoenergeticheskimi sil'notochnymi elektronnyimi puchkami* (Modification for Surface Layers of Metal Materials by Low-Energy High-Current Electron Beams), Novosibirsk: Nauka, 2019.
7. Ozur, G.E. and Proskurovskii, D.I., *Plasma Phys. Rep.*, 2018, vol. 44, no. 1, p. 18. <https://doi.org/10.1134/S1063780X18010130>
8. Nazarov, D.S., Ozur, G.E., and Proskurovskii, D.I., *Instrum. Exp. Tech.*, 1996, vol. 39, no. 4, p. 546.
9. Abdullin, E.N., Ivanov, N.G., Losev, V.F., and Morozov, A.V., *Laser Part. Beams*, 2013, vol. 31, p. 1. <https://doi.org/10.1017/S026303461300075X>
10. Bugaev, A.S., Klimov, A.I., Koval', N.N., Koshelev, V.I., Sochugov, N.S., and Shchanin, P.M., *Preprint of Tomsk Scientific Center of the Siberian Branch USSR Acad. Sci.*, Tomsk, 1991, no. 25.
11. Kovalchuk, B.M., Polevin, S.D., Tsygankov, R.V., and Zherlitsyn, A.A., *IEEE Trans. Plasma Sci.*, 2010, vol. 38, no. 10, p. 2819. <https://doi.org/10.1109/TPS.2010.2060367>
12. Engelko, V.I., Kuznetsov, V.S., and Mueller, G., *J. Appl. Phys.*, 2009, vol. 105, p. 023305. <https://doi.org/10.1063/1.2996286>
13. Engel'ko, V.I., Tkachenko, K.I., Rusanov, A.E., and Birzhevoi, G.A., *Vopr. At. Nauki Tekh., Ser.: Yad.-Reakt. Konstany*, 2015, no. 4, p. 93.
14. Breizman, B.N., Ryutov, D.D., and Stupakov, G.V., *Izv. Vyssh. Uchebn. Zaved., Fiz.*, 1979, no. 10, p. 7.
15. Kiziridi, P.P. and Ozur, G.E., *Tech. Phys. Lett.*, 2020, vol. 46, no. 8, p. 775. <https://doi.org/10.1134/S1063785020080088>
16. Petrov, V.I., Kiziridi, P.P., and Ozur, G.E., *Zh. Tekh. Fiz.*, 2021, vol. 91, no. 11, p. 1764. <https://doi.org/10.21883/JTF.2021.11.51541.80-21>
17. Kesaev, I.G., *Katodnye protsessy elektricheskoi dugi* (Cathode Processes of Electrical Arc), Moscow: Nauka, 1968.
18. Mesyats, G.A. and Proskurovskii, D.I., *Impul'snyi elektricheskii razryad v vakuume* (Pulse Electrical Discharge in Vacuum), Novosibirsk: Nauka, 1984.
19. Rotshtein, V.P., Ivanov, Yu.F., Markov, A.B., Proskurovsky, D.I., Karlik, K.V., Oskomov, K.V., Uglov, B.V., Kuleshov, A.K., Novitskaya, M.V., Dub, S.N., Pauleau, Y., and Shulepov, I.A., *Surf. Coat. Technol.*, 2006, vol. 200, p. 6378.

Translated by A. Seferov